

The *divIVB* Region of the *Bacillus subtilis* Chromosome Encodes Homologs of *Escherichia coli* Septum Placement (MinCD) and Cell Shape (MreBCD) Determinants

A. W. VARLEY¹ AND GEORGE C. STEWART^{2*}

Department of Microbiology, University of Kansas, Lawrence, Kansas 66045,¹ and Department of Microbiology and Immunology, University of South Carolina School of Medicine, Columbia, South Carolina 29208²

Received 4 June 1992/Accepted 7 August 1992

Mutation of the *divIVB* locus in *Bacillus subtilis* causes frequent misplacement of the division septum, resulting in circular minicells, short rods, and filaments of various sizes. The *divIVB1* mutant allele maps to a region of the chromosome also known to encode sporulation (*spo0B*, *spoIVF*, *spoIIB*) and cell shape (*rodB*) determinants. This study reports the cloning and sequence analysis of 4.4 kb of the *B. subtilis* chromosome encompassing the *divIVB* locus. This region contains five open reading frames (ORFs) arranged in two functionally distinct gene clusters (*mre* and *min*) and transcribed colinearly with the direction of replication. Although sequence analysis reveals potential promoters preceding each gene cluster, studies with integrational plasmids suggest that all five ORFs are part of a single transcription unit. The first gene cluster contains three ORFs (*mreBCD*) homologous to the *mre* genes of *Escherichia coli*. We show that *rodB1* is allelic to *mreD* and identify the *rodB1* mutation. The second gene cluster contains two ORFs (*minCD*) homologous to *minC* and *minD* of *E. coli* but lacks a *minE* homolog. We show that *divIVB1* is allelic to *minD* and identify two mutations in the *divIVB1* allele. Insertional inactivation of either *minC* or *minD* or the presence of the *divIVB* region on plasmids produces a severe minicell phenotype in wild-type cells. Moreover, *E. coli* cells carrying the *divIVB* region on a low-copy-number plasmid produce minicells, suggesting that a product of this locus may retain some function across species boundaries.

With few exceptions, procaryotes multiply by binary fission. Strict spatial and temporal regulation is needed to ensure that division occurs only when the cell reaches a certain critical mass, that septum formation divides the cell into equal halves, and that all essential genetic and biochemical components are properly partitioned. Moreover, the process must be fine-tuned to allow the bacterium to adapt to different growth conditions or to respond to potentially lethal DNA damage.

Most of what is known at the genetic level about binary fission has been learned by studying the gram-negative rod *Escherichia coli*. Molecular techniques have allowed the identification of several critical components of the division apparatus and led to the development of a tentative model of how these components interact (10, 28). Several lines of evidence suggest that the *ftsZ* gene product plays a pivotal role as a positive effector of cell division. Significantly, FtsZ has been shown to localize at the newly formed septum (5).

FtsZ also is the target of division inhibitors from at least two separate regulatory pathways (14), one of which, *minB*, appears to be the principal determinant of septum placement (13). Mutation at this locus leads to the formation of circular, anucleate cells (minicells) through placement of the division septum near the cell pole (1). The *minB* locus has been cloned and characterized, and the interactions of its products have been worked out in some detail. Two of its products (MinC and MinD) work together to inhibit septation at all potential sites, while a third (MinE) confers specificity on MinCD by preventing inhibition at the central septation site (13). MinC appears to be the inhibitory com-

ponent, since overexpression of *minC* alone causes filamentation and since MinC can also function as a division inhibitor in association with DicB (14, 25). MinD plays an accessory role, enhancing the inhibitory effect of MinC and allowing interaction with MinE (14). Consistent with a regulatory function, MinD has also been shown to have ATPase activity (11). How MinE confers specificity on the MinCD inhibitor is unclear. Indeed, little biochemical evidence on the mode of action of any of these gene products exists.

Cell division genes from gram-positive organisms have not been as well studied. The *Bacillus subtilis* homolog of *ftsZ* has been cloned and shown to be essential for septation during both vegetative growth and sporulation (3). Nucleotide sequence analysis has also revealed that FtsZ shows a high degree of amino acid sequence similarity to FtsZ of *E. coli* (2, 7). Consistent with a conservation of structure and function, overexpression of the *Bacillus* homolog in *E. coli* causes a lethal filamentation which can be overcome by increasing expression of the *E. coli* gene (2).

Two loci which are associated with a minicell phenotype have been identified in *B. subtilis* 168: *divIVA*, located at 144° on the genetic map, and *divIVB*, located at 245° (33). Mutation at the *divIVB* locus results in aberrant placement of the division septum leading to a minicell phenotype formally analogous to that seen in *E. coli minB* strains. In *divIVB1* strains, misplacement of the division septum occurs frequently, with as many as three of every four divisions being aberrant (33). Most typically, the septum forms near one pole of the cell, resulting in a small, circular minicell which lacks chromosomal DNA and is incapable of growth or division (33). Misplacement of the septum between the polar region and the normal division site also occurs, generating

* Corresponding author.

oval cells and short rods of various sizes. Apparently, a range of cell sizes is possible, suggesting that the septum may form anywhere within a zone at the central or polar septation sites. Short rods formed in this way have been reported to occasionally divide, even though they lack chromosomal DNA and do not grow (33).

In this paper, we report the cloning and sequencing of the *divIVB* region of *B. subtilis*. This region contains five open reading frames (ORFs) which can be grouped into two gene clusters based on function but which appear to be transcribed as a single unit. The downstream gene cluster is shown to be the *divIVB* locus and contains two genes whose products show significant amino acid homologies to MinC and MinD of *E. coli*. The *divIVB1* mutant allele is mapped to *minD*, and the mutations are identified. Significantly, the *divIVB* locus lacks a *minE* homolog. Upstream of the *divIVB* locus is a second gene cluster homologous to the *mre* locus of *E. coli*. *mreD* is shown to be allelic to *rodB*, and the *rodB1* mutation is identified.

MATERIALS AND METHODS

Bacterial strains and bacteriophages. Lambda gt-wes DNA was obtained from Bethesda Research Laboratories. Lambda gt-wes phage was obtained by transfection of *E. coli* with this DNA.

The wild-type strain used in this study was *B. subtilis* 168 *trpC2* (21). CU403 (*divIVB1 thyA1 thyB1 metB5*) (33) and ROD104 (*leuA8 rodB1*) (23) were obtained from John Reeve and the *Bacillus* Genetic Stock Center (The Ohio State University), respectively. Strain CU403 exhibits unsatisfactorily low levels of competency for genetic transformation. To place the *divIVB1* marker into a more suitable background, KUS1101 was created by transforming JH642 (*pheA1 trpC2*) (9) with chromosomal DNA from CU403 and selecting for *pheA*⁺ *divIVB1* transformants by plating on minimal medium (42) with tryptophan followed by microscopic screening of individual colonies for minicells. A single clone was picked, and the *divIVB1* marker was verified by repeating the genetic mapping to *pheA*. The resulting strain became highly competent and was used for all subsequent manipulations involving *divIVB1*.

General methods. Media and growth conditions, including antibiotic concentrations, used for the propagation and selection of *E. coli* and *B. subtilis* were as described previously (21).

B. subtilis was made competent and transformed by the method of Erickson and Copeland (16). Manipulation of plasmid and phage DNA in *E. coli* was performed as described by Sambrook et al. (35). Isolation of chromosomal and plasmid DNAs in *B. subtilis* was performed as described previously (21, 33).

Determination of the *divIVB1* phenotype and photomicrography. Cells were screened for minicells essentially as described by deBoer et al. (12). *B. subtilis* cultures were grown at 37°C with vigorous agitation to late log phase and concentrated in saline to 1/10 of the original volume. Cells for photomicrography were first washed and concentrated and then fixed in 0.5% glutaraldehyde for 15 min. Volumes (5 µl) were transferred to slides previously coated with poly-L-lysine, and phase contrast micrographs were taken with Kodak TMY-400 film.

Cloning in lambda gt-wes. Large-scale preparation of lambda DNA and preparation of lambda arms were carried out as described by Sambrook et al. (35). Insert DNA was prepared by digesting *B. subtilis* 168 chromosomal DNA to

completion with *EcoRI* and then size fractionating it on a 10 to 40% sucrose gradient. Aliquots of individual fractions were electrophoresed on a 0.8% agarose gel, transferred to nitrocellulose filters, and probed with the insert from pAV2174. Hybridizing fractions were pooled and used as insert in ligation and packaging reactions as specified by the manufacturer of the commercial Packagene kit (Promega).

Cloning of the *divIVB* region. Genetic mapping studies (33) placed *divIVB* between *spo0B* and *rodB*. In previous studies, we had constructed two strains containing plasmids integrated into the chromosome of *B. subtilis* 168, pAV31ΔPst in the *spo0B* region and pAV2174 in the *spoIIB* region (38). To further localize *divIVB* relative to these strains, we performed physical mapping experiments with the inserts of the integrated plasmids as hybridization probes. Since the integration of the plasmids introduced an additional *BamHI* site, we were able to determine that the two probes hybridized to the same 15-kb *BamHI* fragment (data not shown). Moreover, aligning the deduced fragment sizes with each other and with previously published physical mapping data from the *pheA* region (17) indicated that the insertion sites were 6 to 8 kb apart. To determine which end of this region contained *divIVB*, we used chromosomal DNA from the insertion strains to determine the cotransformation frequency of the Cm^r marker and the *divIVB* wild-type allele of the insertion strains by transformation of KUS1101 (*divIVB1*). The results indicated that *divIVB* was approximately equidistant from the two insertions and would therefore be located on the 6-kb *EcoRI* fragment to which pAV2174 hybridized.

To clone this fragment, we constructed a collection of recombinant lambda phages containing *EcoRI*-digested *B. subtilis* 168 chromosomal DNA as described above. A recombinant phage (gtAV16.2) carrying the expected 6-kb *EcoRI* insert was identified by plaque hybridization (4) with the insert from pAV2174 as end-labeled probe. A 3.9-kb *BglII* fragment of this phage hybridizing to the insert of pAV2174 was subcloned into the *BamHI* site of the pSC101-based low-copy-number plasmid pCL1921 (26) to yield pAV2145. In order to provide a marker selectable in *Bacillus* spp., the chloramphenicol acetyltransferase (CAT) cassette from pER919a (34) was subcloned into the vector portion of pAV2145 at the *EcoRI* site to create pAV2148. Plasmid pAV2148 was integrated into the chromosome of KUS1101 (*divIVB1*) by transformation and then selected on chloramphenicol. Transformants were screened microscopically as described above and found to have complemented the *divIVB1* phenotype (see Fig. 8A, B, and C), though small numbers of minicells were observed. The reason a slight minicell type results from integration of pAV2148 is discussed below.

Other plasmid constructions. Plasmids pAV2176 and pAV2177 were constructed by subcloning the insert from pAV2145 into the shuttle plasmid pMK4 (37) and the *B. subtilis* low-copy-number plasmid pHP13 (20), respectively, using the flanking *EcoRI* and *SalI* sites in the multiple cloning site of pAV2145. Plasmids pAV2217, pAV2218, and pAV2219 were constructed by subcloning the leftward, central, and rightward *HindIII*-*PstI* fragments, respectively, from pAV2176 (Fig. 1A) into pUC18 and then inserting the CAT cassette.

The inserts of integrational plasmids used in this study are shown in Fig. 1A and C, with the vertical marks aligning with the restriction endonuclease sites (Fig. 1B) used for subcloning. After digestion with appropriate restriction endonucleases, inserts were isolated by gel purification with Gene-

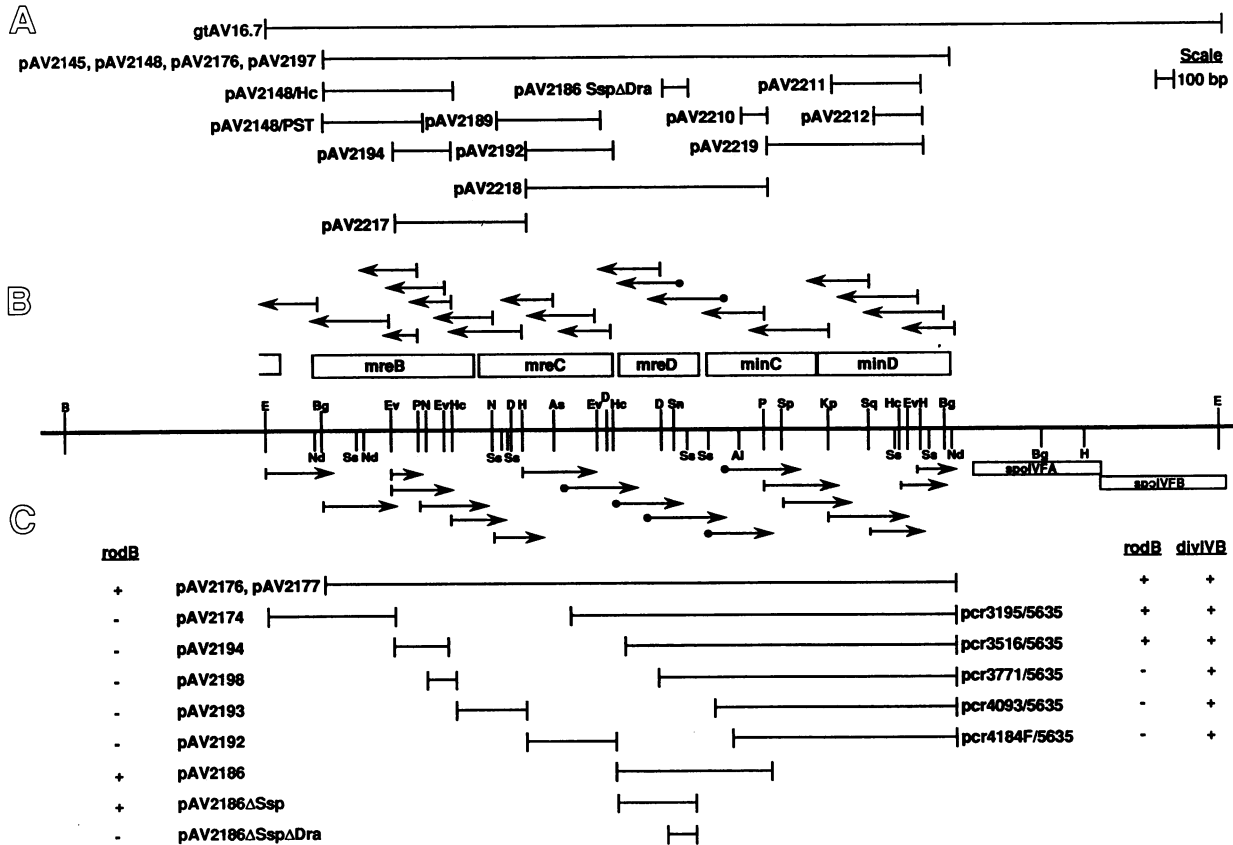


FIG. 1. Physical map of the *divIVB* region of *B. subtilis* 168. (A) Locations of the inserts of phage gtAV16.2, in which the *divIVB* region was cloned, and of the plasmids used in complementation and insertional inactivation of the *mre-min* genes. The vertical lines at the end of the inserts are positioned directly above the restriction endonuclease sites on the physical map (B) used in cloning. (B) Physical map of the region and the strategy used to sequence it. Vertical marks above the line show the locations of restriction endonuclease sites used in subcloning; marks below the line show other landmarks mentioned in the text. Arrows above and below the physical map represent the directions and extents of individual sequencing determinations (performed in duplicate). Symbols at the beginning of each arrow indicate whether the sequencing start point was a restriction site (vertical bar) or a synthetic oligonucleotide (filled circle). Rectangles above the map show the positions and extents of the ORFs identified by our sequencing. Rectangles below the line represent ORFs obtained from the sequence of the *spoIVF* region published by Cutting et al. (8). All of these ORFs are transcribed in the same direction (left to right). (C) Locations of the plasmid inserts (left) and PCR products (right) used to map the *rodB1* and *divIVB1* mutations. The results of complementation analyses are indicated next to each insert or PCR product as + (complementation) or - (no complementation) under the appropriate allele designation (*rodB* or *divIVB*). Restriction endonuclease sites are abbreviated as follows: Al, *AluI*; As, *AseI*; B, *BamHI*; Bg, *BglIII*; D, *DraI*; E, *EcoRI*; Ev, *EcoRV*; H, *HindIII*; Hc, *HincII*; Kp, *KpnI*; N, *NotI*; Nd, *NdeI*; P, *PstI*; Sa, *SacI*; Sn, *SnaBI*; Sp, *SphI*; Ss, *SspI*.

Clean II (Bio 101) and then ligated to pUC18 cleaved with the same restriction endonucleases used to generate the insert (sticky ends) or with *HincII* (blunt ends). Selection for Campbell-type insertion was provided by subcloning the CAT cassette into the *EcoRI* site of the pUC18 linker.

Sequencing strategy. The strategy used to sequence the *divIVB* region is shown in Fig. 1B. All sequencing was done by the dideoxy termination method of Sanger et al. (36) with Sequenase (United States Biochemical) and according to the protocols supplied by the manufacturer. Three sources of template were used. Most of the region between the *BglIII* sites was sequenced by subcloning of restriction fragments from pAV2176 into the phage vectors M13mp18 and M13mp19 followed by single-stranded sequencing of duplicate clones. Where possible, the replicative forms of the larger phages were used to create subclones by deleting restriction fragments from the ends of the inserts. Junctions of nonoverlapping M13 clones were sequenced by subclon-

ing of restriction fragments from pAV2176 into the plasmid pUC18 followed by double-stranded sequencing. The region between nucleotides 1920 and 2910 (Fig. 2) was sequenced with the aid of primers obtained from Genosys Inc. or the University of South Carolina Oligonucleotide Synthesis Facility. All oligonucleotides used in this study are named according to their 5'-3' nucleotide positions in Fig. 2. Those bearing the designation C following their coordinates are complementary to the sequence in Fig. 2; otherwise, they are identical.

The region downstream of the *BglIII* site in *minD* was sequenced by using single-stranded templates generated by the polymerase chain reaction (PCR). To prime the lower strand (Fig. 1B), we designed an oligonucleotide (pr4197-4212) based on sequence generated as described above. To prime the upper strand, we designed an oligonucleotide (pr4363-4377C) from sequence previously published by Cutting et al. (8). Symmetric PCR was carried out with these

EcoRI
 GAATTCATCTATTGTCACCCCGGAGAGGTGTTAAAGAAGCGTTAAACGATCTGCCGCTTCCTTTATCTGTGTTTATAATCATCCTTCTGGAGATCCG 100
 N S S I V H P R E V F K E A F K R S A A S F I C V H N H P S G D P

 ACGCCGAGCAGGGAAGATATTGAAGTGACAAGACGSCGTGTTGAATGCGGAAACCTGATTGGCATCGAGCTGCTTGACCATTGGTGATCGGGGATAAAA 200
 T P S R E D I E V T R R L F E C G N L I G I E L L D H L V I G D K K

 AATTTGTGAGTTTAAAGGAAAAAGGATATTGTAACACTTTTTTCGTGCAATTAAGCTATAATAGAGTTTATGAGTTTTCCCTTTAGGGTATTTTTG 300
 F V S L K E K G Y L *

 CTTTAAAGAAAGGAAGATACATATGTTTGAATTGGTGTAGAGACCTTGGTATAGATCTTGGAACTGCGAATACGCTTGTTTTGTAAAGGAAAA 400
 rbs mreB M F G I G A R D L G I D L G T A N T L V F V K G K

 GGAATTGTTGTGAGAGAGCGCTCAGTTGTGCTTTCGAGACGGATACGAAATCGATTGCTGCTCGGAAATGATGCGAAAAATATGATTGGACGGACAC 500
 G I V V R E P S V V A L Q T D T K S I V A V G N D A K N M I G R T P

 CGGGCAACGTGGTGGCTCTTCGCCCGATGAAAGACGGCGTTATCGCTGATTGAAACAACGGCAGCATGATGAAATATTACATCAATCAGGCCATAAA 600
 G N V V A L R P M K D G V I A D Y E T T A T M M K Y Y I N Q A I K

 AAATAAAGGCATGTTTCCAGAAAACCATATGTAATGGTATGTGCCATCAGGCATTACAGCTGTTGAAGAACGGCGTGTATCGATCGACAAGACAG 700
 N K G M F A R K P Y V M V C V P S G I T A V E E R A V I D A T R Q

 GCGGGAGCGCTGACGCGTATCCGATTGAAGACGCTTTGCCGACGAAATCGCGCAATTCGCCAGTTGGGAACCGACTGGAAGCATGGTTGTTGATA 800
 A G A R D A Y P I E E P F A A A I G A N L P V W E P T G S M V V D I

 TCGGGGCGGTACGACAGAAGTTCGATTATCCCTCGGAGGCATCGAACGCTCAGTCAATCCGTGTAGCCGGTGTAGATGGATGACGCGATTAT 900
 G G G T T E V A I I S L G G I V T S Q S I R V A G D E M D D A I I

 CAACTACATCAGAAAACGTACAATCTGATGATCGGTGACCTACGGCTGAAGCGATTAATAATGGAATCGGATCTGCAGAAAGCTCCTGAAGAATCCGAC 1000
 N Y I R K T Y N L M I G D R T A E A I K M E I G S A E A P E E S D

 AACATGGAATCCGCGGCCGCGATTGCTCACAGGTTTCCGAAAACAATTGAAATTACAGAAAAGAGATTCTAACGCTCTACCGCAGACTGTATCTA 1100
 N M E I R G R D L L T G L P K T I E I T G K E I S N A L R D T V S T

 CAATTGTCGAAGCAGTGAAGAGCACACTCGAAAAAACCCGCTGAGCTTCGACGAGATATCATGGACAGAGGTATAGTGTAAACGGCGCGGGAGCGCT 1200
 I V E A V K S T L E K T P P E L A A D I M D R G I V L T G G G A L

 TTTGCGCAATTTGGACAAAGTCATCAGCGAAGAAACAAAAATGCCGGTCTTATCGCCGAAGATCCGCTTGATTGTGATAGCGATCGGAACAGGGAAGCA 1300
 L R N L D K V I S E E T K M P V L I A E D P L D C V A I G T G K A

 CTGGAGCACATCCATCTTTCAAAGGAAAAACTAGATAATCGGGAGTTCATAGAGAGGTGTAACACGATGCCGAATAAGCGGTTAATGCTATTACTTC 1400
 L E H I H L F K G K T R *

 TGTGATTATCATATTGGTGGCTATGATTGGATTTTCGCTGAAGGGCGGCCGCAATACCCTGGCCTGAGAAAAGTATCGCGGATACGACGGGAGTATT 1500
 C I I I L V A M I G F S L K G G R N T T W P E K V I G D T T G V F

 TCAAAATATTTTTCATACGCTGCCGAATTTTTCGAGGAATTTTGAAGAACATCAATGATTTTAAAAAACACATACAAAAGAAAACGAGCGTCTAAGAGAA 1600
 Q N I F H T P A E F F A G I F E N I N D L K N T Y K E N E R L R E

 AAACCTGACGGACAGACACAATGAAGCCAAAGCTTCAAGAGCTTGAAGAGAAAACAAATCCTTGCCTGACGAGCTTGGCCATGTCAAATCGATTAAG 1700
 K L D G Q T Q Y E A K L Q E L E E E N K S L R D E L G H V K S I K D

 ATTACAAGCCGATTTAGCAACGGTCATCGCCAGAAGCCCTGATAATTTGGCGAAGACAGGTACCATTAAACAGGGGACTCAGCAAACCTAGCGAAAAGA 1800
 Y K P I L A T V I A R S P D N W A K Q V T I N K G T Q Q N V A K D

 TATGGCCGTTACAACGAAAAGGCGCATTAAATCGGCAAGATCAAAGCTCCGACTTAACAATTTTACGTTGCTGTTTCAAGCATTAAAGCATTACTGAC 1900
 M A V T N E K G A L I G K I K S S G L N N F T S A V Q L L S D T D

 CGCAATAACAGAGTCGCGACAAAAATTTCCGAAAAAAGGCGAGCAAGGCTACGCTTGTGCGAAGGATGACAAAAGAAAAACGCTTAAAGATGA 2000
 R N N R V A T K I S G K K G S K G Y G L I E G Y D K E K K R L K M T

 CAATTATTGAGCGTAAGGATAAAACAAGACGTGAAAAAGGCGATCTTATTGAAACATCAGGGACAGGCGGTGTTTTCCCAAGGGCTGACAATCGGTGA 2100
 I I E R K D K Q D V K K G D L I E T S G T G G V F P E G L T I G E

 AGTGACTGATATCGAGTCAGATTCCTATGGATTAACGAAGTTGCTTATGTAACCTCGGGCTGACCTTACAGATTTAAATAATGTGATCGTTGTTAAC 2200
 V T D I E S D S Y G L T K V A Y V K P A A D L T D L N N V I V V N

 CGTGACGTGCCGACTGTGCATACAGAGGAGGAAGGATCGTGAACGTTTCTTCTCCCTTCGTTATGATGCTTGTGTTTTTCTCGGAAAGCATTTTTAC 2300
 R D V P T V D T E E E G S *

 AGATTTGGTGATTTTCTTTCGTTACAGATGACCAAGTCTCGCCCGCTTTTTTGTGCTTGTATTGATTCATGTGCGGCTTTTATCAACAAAAA 2400

FIG. 2. Nucleotide sequence of the nontranscribed strand of the *divIVB* region. The translated polypeptide is shown below the nucleotide sequence, with the one-letter designation of each amino acid residue positioned below the first nucleotide of the codon. Putative ribosome-binding sites are underlined and indicated (below the translated product) (rbs). Start codons are preceded by the name of the ORF, and stop codons are indicated by asterisks. A putative rho-independent terminator distal to *minD* is indicated by double underlining of the nucleotide sequence of the inverted repeat. A potential nucleotide-binding fold in *minD* is identified by double underlining of the amino acid sequence. Nucleotides are numbered from the start of the *EcoRI* site.

D L V H F P F V T D D Q V L A P R F L M L V L I F M S A F I N Q K
CACGCGATGATTTACGGATTTATTTTGGCTTCTATATGACATGAACATACAGTCTATTAGCGTTTACATGTTTGGTTTTGACGGGCTATGCTATT 2500
H A M I Y G F I F G F L Y D M N Y T S L L G V Y M F G F A G L C Y L
TGGCTTCAAAGCGTTTAAAGTGTGCATACAAACGCATTTGTAGTGATTTGATAGCAGTTCTGGCTGTCTGCTCGAATTTTACGTTATTCGGCAT 2600
A S K A F K V L H T N A F V V I L I A V L A V C L L E F Y V F G I
TCAGTCTTTGATTATAAGACATTATGACGTTTAAACGGATTTGCTGTTGACCGGTTTATACCGACAATTTTATAAATATTGCAGCAGCTCTATTCTT 2700
Q S L I H K D I M T F N G F V L D R F I P T I L L N I A A A L I L
GTTCTGCCATTTAGATTGTTTTTATGAGTCTAAAGAAAGATTGAGAGATGAGTAAAAAGGATTTTATCTTTTTTGGACGAATGAGTATGTTGTTGAG 2800
V L P F R L F F M S L K K E L R D E * rbs
SspI
GTGAATTTGTGAAGACCAAAAAGCAGCAATATGTAACAATAAAAGGAACAAAGAAATGGACTAACATTGCATCTGGATGATCGGTGTTCTTTTGTAGAGC 2900
minC M K T K K Q Q Y V T I K G T K N G L T L H L D D A C S F D E L
TTCTCGATGGTCTTCAGAATATGCTGTCAATTGAACAATATACCGATGAAAAGGCCAGAAAATCAGCGTTCATGTTAAGCTGGGAAATCGCTTTTATA 3000
L D G L Q N M L S I E Q Y T D G K G Q K I S V H V K L G N R F L Y
TAAGGACGAGGAAACAGCTAACCGAATGATTGCGTCAAAGAAAGATTGTTGTTCTATTGACAGTGAAGTCATTACTAAAAAGAAAGCAGACAG 3100
K E Q E E Q L T E L I A S K K D L F V H S I D S E V I T K K E A Q
PstI
CAGATAAGAGAGGAAAGCCGAAATTTTCTGTTTCAAATTTGCTGTTTCAAGGCAAGTCTGCAGGTAAGGCGACTTCTCCTGATCGGTGACGTGA 3200
Q I R E E A E I I S V S K I V R S G Q V L Q V K G D L L L I G D V N
FspI SphI
ATCCCGCGGAAACAGTCAAGGCGGAGGAAACATTTTGTCTGGGCTCACTGAAAGAAATGCGCATGCTGGATTCAATGGAAATAATCAAGCGGTAT 3300
P G G T V R A G G N I F V L G S L K G I A H A G F N G N N Q A V I
CGCCGCTCTGAAATGCTCCGACACAATTAAGAATCAATCATGTGTTAAATCGCTCCCCAGACCACATTCAAAAGGAAACGAAATGGAATGTGCTTAT 3400
A A S E M L P T Q L R I N H V L N R S P D H I Q K G N E M E C A Y
TTAGATACAGACGAAATATGGTCATTGAACGCCTTCAACATTTGGCTCATTTAAGACCTGATCTAACAGGCTTGGGGAGGAATGTGAATGGGTGAG 3500
L D T D G N M V I E R L Q H L A H L R P D L T R L E G G M * M G E rbs minD
KpnI
GCTATCGTAATAACTTCGGGAAAAGCGGAGTAGGTAAGACAACAACATCTGCGAACCTCGGTACCGCTTAGCCATTTTAGGGAAGCGGTATGCTTAG 3600
A I V I T S G K G G V G K T T T S A N L G T A L A I L G K R V C L V
FspI NsiI
TAGATACTGATATAGGACTGCGCAACCTTGATGTTGAATGGGTCTTGAATAAGAAATATTACGATCTGGTAGAGCTGTAGAGGGCAGATGCAAAAT 3700
D T D I G L R N L D V V M G L E N R I I Y D L V D V V E G R C K M
PvuII
GCATCAGGCGCTCGTAAAAGACAACAGTTTCGATGATCTGCTCTATTTAATGCCCGCTGCTCAAACGAGCGATAAGACAGCTGTTGCTCCTGAACAAAT 3800
H Q A L V K D K R F D D L L Y L M P A A Q T S D K T A V A P E Q I
SacI
AAAACATGGTCAAAGAGCTCAAACAGGAATTTGACTATGTCATCATAGACTGCTCCTGCCGGAATCGAGCAAGGGTACAAAAATGCCGTTTCCGGAGCTG 3900
K N M V Q E L K Q E F D Y V I I D C P A G I E Q G Y K N A V S G A D
PvuII SspI SacII
ATAAAGCGATTGGTCACTACGCTGAAATCTCAGCTGTTGCTGATGCTGACCGTATTATAGGACTGCTGGAGCAAGAGGAAATATGAACCGCGCGG 4000
K A I V V T T P E I S A V R D A D R I I G L L E Q E E N I E P V
HpaI/HincII EcoRV PvuI ClaI
GCTCGTGTAAACAGAAATCAGAAATCACCTGATGAAAACGGTGACACGATGGATATCGACGAAATCGTACAGCATCTGTCGATCGATTGCTCGGAATC 4100
L V N R I R N H L M K N G D T M D I D E I V Q H L S I D L L G I
HindIII SspI
GTGGCTGATGATGATGAAGTCATTAAAGCTTCCAATCATGGCGAACCGATTGCGATGGACCTAAAAACCGCTTCCATTGCATATCGCAATATTGCC 4200
V A D D D E V I K A S N H G E P I A M D P K N R A S I A Y R N I A R
BglII
GCCGCATCTTAGGTGAATCTGTTCTTTACAGGTGCTTGAAGAGCAAAAACAAAGGAATGATGGCTAAGATTAAAGCATTTCGGAGTAAGATCTTAATG 4300
R I L G E S V P L Q V L E E Q N K G M M A K I K S F F G V R S *
NdeI
TGATAGAATCAAAGAGAAGAAATCTGACAAGCATATGCTGTGTCAGGTTTTTTTTGTTTTGCTGCTTGTCTTACTAAACCGAAT 4389

FIG. 2—Continued.

primers and template DNA prepared from phage gtAV16.2. The product was then amplified for single-stranded sequencing by asymmetric PCR (22). The products from three separate symmetric-PCR amplifications were sequenced in this way.

The putative polypeptide products of all ORFs were compared to the EMBL, SWISS-PROT, GenPept, and GenBank data bases by using the FASTA comparison routine of Pearson and Lipman (32).

Complementation analyses of the *rodB1* and *divIVB1* mutant alleles. To localize the *rodB1* mutation, the complementation analysis shown in Fig. 1C was performed by making use of the observation that *rodB1* exhibits a temperature sensitivity phenotype (6). Plasmid DNA (Fig. 1C, left) or PCR product (Fig. 1C, right) was transformed into competent ROD104

(*rodB1*) cells, plated on tryptic soy agar, and incubated overnight at 55°C. Complementation was determined by growth at the nonpermissive temperature and was verified by phase-contrast microscopy.

Attempts to map the *divIVB1* mutation with integrational plasmids overlapping the 5' end of the *min* locus failed (see Results). To avoid possible polar effects on the *min* genes by Campbell insertion of plasmids, complementation by conjugation was performed. KUS1101 competent cells were transformed with 100 ng of pMK4 and 1 µg of PCR product per ml. After selection for plasmid-encoded Cm^r, transformants were screened for wild-type colonies (smaller, whiter) and verified by phase-contrast microscopy. Under these conditions, a PCR product spanning all of *minC* and *minD* complemented at 0.5%.

Strategy for sequencing the *rodB1* and *divIVB1* mutant alleles. To sequence the *rodB1* mutant allele, chromosomal DNA from strain ROD104 was used for symmetric PCR amplification of the region between primers pr1906-1920 and pr2893-2910C, and template for sequencing was generated by asymmetric PCR. The entire *rodB1* mutant allele was then sequenced by using this template and primers pr1906-1920, pr2227-2241, pr2481-2496, pr2803-2818 (bottom strand), pr2893-2910C, and pr2595-2610C (top strand). To eliminate the possibility that the *Taq* polymerase had introduced the observed base changes, three different symmetric-PCR reactions were used to generate sequencing templates.

To sequence the *divIVB1* mutant allele, the entire *min* gene clusters of both KUS1101 and CU403 were amplified by symmetric PCR with primers pr2481-2496 and pr4362-4377C. Products from three symmetric amplifications (per strain) were then used as template for asymmetric-PCR amplification with primer pr4362-4377C. All three asymmetric-PCR products were sequenced by using primers pr2803-2818, pr2893-2910, pr3293-3307, pr3687-3701, and pr4197-4212. To sequence the opposite strands, the regions containing the observed mutations were cloned from the symmetric-PCR products in duplicate into pUC18 and subjected to double-stranded sequencing as described previously.

Nucleotide sequence accession number. The nucleotide sequence shown in Fig. 2 has been deposited with GenBank under accession number M95582.

RESULTS

Organization of the *divIVB-rodB* region. We sequenced a region of the *B. subtilis* 168 chromosome spanning 4.4 kb from an *EcoRI* site to 90 bp downstream of the rightward *BglII* site in pAV2145 (Fig. 1B). The region contains five ORFs oriented colinearly with the direction of replication and arranged in two functionally distinguishable gene clusters (*mre* and *min*). Upstream of the first gene cluster, our sequence overlaps the 3' end of a previously sequenced transcription unit containing two ORFs (6). Following this transcription unit is a noncoding region of 93 bp which sequence analysis and preliminary promoter probe studies (38) suggest contains promoter activity, but the precise location and extent of this promoter activity have not been determined. The first gene cluster (*mre*) begins just upstream of the leftmost *NdeI* site and contains three ORFs (*mreBCD*) spanning approximately 2.44 kb (nucleotides 320 to 2757, Fig. 2). The second gene cluster (*min*) is positioned immediately downstream of the *mre* genes with no obvious transcriptional terminators between them. However, a potential promoter precedes the *min* gene cluster with its -35 region overlapped by the last four codons of *mreD*. This potential promoter is homologous in sequence and spacing (TTGAgA, nucleotides 2743 to 2748; TATctT, nucleotides 2767 to 2772; Fig. 2) to the class of promoters recognized by σ^A -bearing RNA polymerase (29). The *min* gene cluster comprises two ORFs (*minCD*) spanning 1.49 kb (nucleotides 2810 to 4298; Fig. 2). Beginning 33 bp downstream of the translational stop codon of *minD* is a region of dyad symmetry (CTGACAAAGC, nucleotides 4323 to 4332; GCTgT GTCAG, nucleotides 4337 to 4346; Fig. 2) capable of forming the stem-loop structure characteristic of rho-independent transcriptional terminators. This sequence, as previously reported by Cutting et al. (8), lies approximately 100 bp upstream of the start codon of *spoIVFA*.

Nucleotide sequence analysis of the *mre* gene cluster. The first ORF of the first gene cluster (*mreB*) begins with an ATG

E. c.	MLKKFRGMSNDLSIDLGTANTLIYVKGQGVILNEPSVVAIRQDRAGSPKSVAAVGH DANEMLGR	
B. s.	M---F-GIGARDLIGIDLGTANTLIVFKGKGIWREPSVALQTD---TKSTVAVGNDARKMIGR	
B. c.	M---F---ARDIGIDLGTANVLIHVKGKGIWLEPSVVAIDRN---TGKVLAVGEEARSVMGR	
E. c.	TPGNIAAIRPMKDGVIADFFVTEKMLQHFIKQ-VHSNS-FMRPSRVLVCPVGTQVERRAIRE	
B. s.	TPGNVVALRPMKDGVIADYETATMKNYINQAIKKNKGFARK-PYVHVCPVSGITAVEERAVID	
B. c.	TPGNIVAIRPLKDGVIADFEITAMLKYFINKLDVKS--FFSKPRIL-ICCPNTITSVEQKAIRE	
E. c.	SAQGAGAREVFLIEEPMAAIGAGLPVSEATGSHVVDIGGCTTEVAVISLNGVTVSSVRIIGDR	
B. s.	ATRQAGARDAYPIEFPAAAGANLPVWEPTGSHVVDIGGCTTEVAIISLGGIVTSQSIRVAGDE	
B. c.	AAERSGGKTVFLEEEPVAAVGAGMEIQPSGNMVDVIGGCTTDIAVLSMGDITVSSSIKMGDK	
E. c.	FDEAIINVYRRNYGLICEATAERIKHEIGSAYPGDEVREIEVGRNLAEGVPRGFTLNSNEILE	
B. s.	MDDAIINIRKTYNLMIGDRTAEAIKMEIGSAPESDNMEIRGRDLLTGLPKTIEITGKEISN	
B. c.	FDMEILNIRKRYKLLIGERTSEDIKIKVGTVPFGAREEELIRGRDVTGLPRTITVCSSEIETE	
E. c.	ALQPLIGIVSVMVALEHTPPELADISERGMVLTGGGLLRNDRLLMEETGIPVVAEDPLT	
B. s.	ALRDTVSTIVEAVKSTLEKTPPELADIMDRGIVLTGGGLLRNDRKVISETKMPVLIADPEID	
B. c.	ALKENAAVIVQAAGVLERTPPELSADIDRGVILTGGGLLHGDMLLAEELKVPVLIENPMH	
E. c.	CVARGGGKALEMIDMHGGDLFSEE	347
B. s.	CVAIGTGKALEHIHLFKGKT-R	337
B. c.	CVAVGTGIMLENIDRLPKRALR	333

FIG. 3. Amino acid similarity between the *MreB* homologs of *E. coli* (E.c.), *B. subtilis* (B.s.), and *B. cereus* (B.c.). Two dots (:) indicate that the residues are identical in opposing proteins; single dots (·) indicate conservative differences. The amino acid sequence of the *B. cereus mreB* gene product is from Narahara et al. (31). The amino acid sequence of the *E. coli* homolog is from Doi et al. (15). Homologies were determined with the FASTA program (32).

codon at position 326 and encodes a protein of 337 amino acids with a molecular weight (MW) of 35,921 (Fig. 2). Immediately upstream is a sequence (AGAAGGAG, nucleotides 306 to 315) with strong complementarity to the 3' end of *B. subtilis* 16S rRNA and properly positioned to serve as a ribosome-binding site (29). The putative product of the *B. subtilis mreB* gene is highly similar to the *mreB* gene products from *E. coli* (15) and *Bacillus cereus* (31). The amino acid sequences of all three genes are aligned in Fig. 3. The *B. subtilis* *MreB* polypeptide shows 52.8% identity to *MreB* of *B. cereus* and 56.8% identity to *MreB* of *E. coli*, with conservative substitutions increasing the similarities to 67.4 and 67%, respectively. The *MreB* polypeptides of *B. cereus* and *E. coli* are 53% identical. Inspection of Fig. 3 also shows that conserved sequences occur in contiguous blocks, with nonconservative changes occurring relatively rarely within them. Where any two products match at a given position, the third is either identical or contains a conservative substitution 85% of the time. Two unconserved regions (residues 76 to 125 and 218 to 266) in which matches among all three polypeptides are relatively rare are apparent. This uniformity of structure is further evident in hydrophathy plots (data not shown), which show two conserved domains (residues 1 to 45 and 140 to 200) of similar extents and hydrophobicities between the two homologs.

The second ORF (*mreC*) of the *mre* gene cluster begins 11 codons downstream of *mreB* (ATG, nucleotide 137) and extends 867 bp, overlapping the putative ribosome-binding site of the third ORF (*mreD*). The predicted product of *mreC* is a polypeptide of 290 amino acid residues with an MW of 32,145. This ORF is preceded by a potential ribosome-binding site (AAGAGGTG) centered 11 bp upstream of the putative start codon (nucleotides 1355 to 1362). The *B. subtilis mreC* polypeptide displays limited similarity to the

B.s.	MPNKRMLLLLLCIIILVAMIGFSLKGGRRNTTWE--KVIGDTTGVFQNIHPTPAEF	54
E.c.	MKPIFSRGPQLIRLILAVLVAL--GIIIIADSRLLGTFQSIRTYMDTAVSPFYFVSNAPREL	59
B.s.	FAGIFENINDLKNTYKENERLREKLDGQQTQYEAQLQEEENKSLRDELGHVKSIDKYK	114
E.c.	LDGVSQTLASRDQLELENRALRQELLLKNSSELLMLGQYKQENARLRELLGSPLRQDEQK-	118
B.s.	ILATVIARSPDNWAKQVTINKGTQQNVAKDMAVTNEKGALIGKIKSSGLNNFTSAVQLLS	174
E.c.	MVTQVISTVNDPYSQVVIDKGSVNGVYEGQPVISDKG--VVGQV--VAVALKTSRVLLIC	175
B.s.	DTDRNRVATKISGKKGSKGYGLIEGYDKEKKRLKMTIIERKDKQDVKKGDLIETSGTGG	234
E.c.	DATHALPIQVL---RNDIRVIAAGNGCTDD---LQLEHL--PANTDIRVGDVLTSLGG	227
B.s.	VFPEGLTIGEVTDIESDSYGLTKVAVYKPAADLTDLNNVIVNRDVTVDTEEEGS	290
E.c.	RFPEGYFVAVVSSVKLDTQRATYVIQARPTAGLRLRYLLLLWGADRNGANFMTPEEVHR	287
E.c.	VANERLQMHPQVLPSPDAMGPKLPEPATGIAQPTFPQPATGNAATAPAAPTQPAANRSP	347

FIG. 4. Amino acid similarities between the MreC homologs of *E. coli* (E.c.) and *B. subtilis* (B.s.). Two dots (:) indicate that the residues are identical in opposing proteins; single dots (·) indicate conservative differences. The amino acid sequence of the *mreC* gene product of *E. coli* is from Wachi et al. (39).

MreC polypeptide of *E. coli* (39), with an identity of 23.2% in a 272-amino-acid overlap (Fig. 4). However, a high number of conservative changes increases the similarity to 68%. Hydrophathy analysis of the two predicted products reveals

that both polypeptides contain a restricted region of strong hydrophobicity near the N terminus (residues 10 to 30) flanked by short regions of hydrophilicity (data not shown). In size, the predicted products of these genes are divergent, with the putative *E. coli* MreC polypeptide being 78 amino acid residues larger (367 amino acids; MW 39,530) (39).

The third ORF (*mreD*) begins at a GTG codon (nucleotide 2239) immediately adjacent to the stop codon of *mreC*. *mreD* spans 513 nucleotides and would encode a polypeptide of 172 amino acid residues with an MW of 19,819. Located entirely within the preceding ORF (*mreC*) is the putative ribosome-binding site (AGAGGAGG, nucleotides 2224 to 2231). The position of *mreD* within the *mre* gene cluster suggested that it would be homologous to the *E. coli* *mreD* gene. Although the two polypeptides are of comparable lengths, the amino acid sequences are quite different (39), with an overall identity of only 21%. Nonetheless, examination of the hydrophathy plots reveals a striking similarity of profile (Fig. 5). The putative products of both genes show five regions of sufficient length and hydrophobicity to be membrane spanning, and the N and C termini of both polypeptides consist of short, strongly hydrophilic stretches of 10 residues each. The overall conservation of the *mre* gene cluster suggests that the similarity in the hydrophobicity profiles of the *B.*

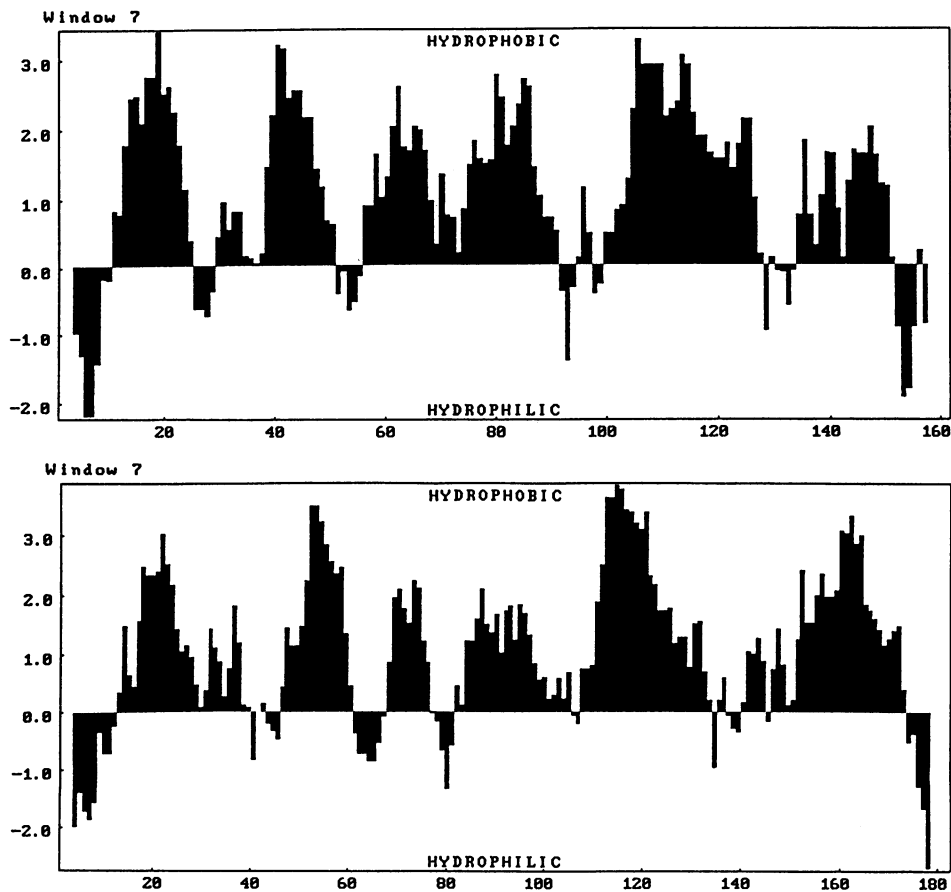


FIG. 5. Comparison of hydrophathy profiles of putative products of the *mreD* genes of *E. coli* (top) and *B. subtilis* (bottom). The strong similarity of the hydrophathy profiles of the two homologs is clear. Both putative products contain five regions of sufficient lengths and hydrophobicities to be membrane spanning. Also evident in both polypeptides are strongly hydrophilic N- and C-terminal domains of 10 residues each. The hydrophathy plot of the *E. coli* homolog was generated by translation of nucleotide sequence from Wachi et al. (39). Hydrophathy analysis was performed as described by Kyte and Doolittle (24).

```

110
B.s. VSKIVRSQQ-BLQVKGDLLIGDVPNGTFRAGGNI FVLGSLKIAHAGFNGNN
E.c. IDTPVRSQRIYAPQCDLIVTSHVSAGAELIADGNIHVYGMHRGRALAGASGDR
130

176
B.s. QAVIAASEMLPTQLRI
E.c. ETQIFCTNLMAELVSI
197

```

FIG. 6. Amino acid similarity between the MinC homologs of *E. coli* (E.c.) and *B. subtilis* (B.s.). Only the sequence of the conserved domain is shown. Two dots (:) indicate that the residues are identical in opposing proteins; single dots (·) indicate conservative differences. The amino acid sequence of the *minC* gene product of *E. coli* is from deBoer et al. (13).

subtilis and *E. coli* MreD polypeptides reflects a conservation of structure and function obscured by the divergence in amino acid sequence.

Nucleotide sequence analysis of the *min* gene cluster. The first ORF (*minC*) of the second gene cluster begins with a GTG codon adjacent to the *SspI* site at nucleotide 2801 and consists of 226 codons whose predicted product has an MW of 25,001. A potential ribosome-binding site (GAGGT) is centered 10 bp upstream of the start codon. Genetic evidence (see below) and position within the gene cluster suggested that this ORF would be homologous to *minC* of *E. coli*. The predicted products of these loci, though similar in length (226 and 231 residues), are divergent in amino acid sequence (13). Overall identity is 17.7%, with conservative substitutions raising total similarity to only 26.1%. A region of significantly greater similarity was identified between amino acid residues 108 and 176, where the two polypeptides are 31.4% identical and 77.1% conserved over a window of 70 residues (Fig. 6).

The second ORF of the *min* gene cluster (*minD*) spans 268 codons and would encode a polypeptide of MW 29,411. The stop codon of *minC* lies between the start codon (TTG, nucleotide 3492) and the putative ribosome-binding site (AGGGAGG, nucleotides 3477 to 3483) of *minD*, raising the possibility that the two genes are translationally coupled (19). This arrangement is also found in the *minB* operon of *E. coli*, except that in the *minB* operon, the stop codon of *minD* lies between the ribosome-binding site and the start codon of *minE* (13). It may be significant in this regard that the *B. subtilis min* locus lacks a *minE* homolog (see below).

The putative products of the *B. subtilis* and *E. coli minD* (13) genes are virtually identical in length (268 and 270 residues, respectively) and very similar. A comparison of the amino acid sequences (Fig. 7) shows that the two polypeptides are identical at 115 of 268 positions (43.7% identity) and contain conservative substitutions at an additional 107 positions (83.3% total similarity). Furthermore, the identical positions are most heavily distributed in the N-terminal two-thirds (residues 1 to 160), with the majority of the nonconserved residues (60%) in the C-terminal one-third (residues 160 to 269). Also located within the conserved region, very close to the N terminus, is a cluster of 11 amino acids identical in sequence and position in both polypeptides (13) and containing a nucleotide-binding consensus sequence (18). Recently, deBoer et al. have shown that *minD* of *E. coli* has ATPase activity (11).

If the *B. subtilis min* locus were strictly homologous to *minB* of *E. coli*, the region immediately downstream of *minD* should contain an ORF corresponding to *minE*. However, three observations indicate that no *minE* homolog is present in this interval: (i) the region could encode only a polypep-

```

B.s. MGEAIVITSGKGGVGGKTTSSANLGTALAILGKRVCLVDTDIGLRNLDVVHGLNRIYDL 60
E.c. MARIIVVTSKGGVGGKTTSSAAIATGLAQKQKKTVIDFDIGLRNLDLIMGERRVYDF 60

B.s. VDVVEGRCKMHQALVKDKRFDDLLYLMPAAQTSDKTAVAPEQIKNMVQELKQ-EFDYVII 119
E.c. VNVIQGDATLNQALIKDKRTEN-LYLPAQSTQTRDKDALTRGVAKVLDLKKAMDFEFIVC 119

B.s. DCPAGIEQGYKNAVSGADKAI VVTTPEISAVRDADRIIGLLE---QEENIEPP---RLV 172
E.c. DSPAGIETGALMALYFADEAIITTNPEVSVSRDSDRILGILASKSRRRAENGEEPIKEHLL 179

B.s. VNRIRNHLMKNGDMDIDEIVQHLSIDLLGIVADDDDEVKASNHGEPIAMDPKNRASIAY 232
E.c. LTRYNPGRVSRGDMLSMEDVLEILRIKLVGVIPEDQSVLRASNGQPEVILDINADAGKAY 239

B.s. RNIAARRILGESVPLQVLEQNKGMMAKISFFGVRS 268
E.c. ADTVERLLGEEPRFRIEEEKGFLKRL--FGG 270

```

FIG. 7. Amino acid similarity between the MinD homologs of *E. coli* (E.c.) and *B. subtilis* (B.s.). The two putative products are nearly identical in length (268 and 270 amino acid residues) and highly conserved throughout (42.9% identity, 82.3% conserved). Two dots (:) indicate that the residues are identical in opposing proteins; single dots (·) indicate conservative differences. The amino acid sequence of the *minD* gene product of *E. coli* is from deBoer et al. (13).

tide of one-third the size of MinE (30 residues versus 88) (13), (ii) all reading frames are closed, and (iii) none of the reading frames encodes a polypeptide with significant similarity to MinE. If *B. subtilis* contains a *minE* homolog, it is located elsewhere on the chromosome.

rodB1 is allelic to *mreD*. Genetic mapping (33) established that *rodB1* is cotransformable with several genes in the *divIVB* region, with the order being *spoIVF-divIVB-rodB-spoIIB*. Wachi et al. (40) had shown that mutation within the *E. coli mre* operon results in a shift in *E. coli* cells from rod shaped to spherical, formally resembling the change exhibited by the *rodB1* mutant. It seemed probable, then, that *rodB1* would be allelic to one of the *B. subtilis mre* genes, and preliminary genetic mapping by R. Losick and coworkers confirmed this expectation (27).

To extend this observation, a series of overlapping clones (Fig. 1C) was constructed and tested for the ability to complement *rodB1*. Since plasmids were found to integrate into the *B. subtilis* chromosome at a low frequency in this region, competent ROD104 cells were transformed with these clones and complementation was tested by growth at the nonpermissive temperature (see Materials and Methods). This method of complementation allowed replacement of the mutant with the wild-type allele by a double-crossover event, avoiding the necessity for a Campbell-type insertion.

Confirming that *rodB1* was allelic to one of the *mre* genes, a plasmid carrying the entire *mre-divIVB* region (pAV2176) complemented the *rodB1* mutation, while PCR products containing only the *min* locus did not (Fig. 1C). Plasmids containing only *mreB* and *mreC* (pAY2175, pAV2194, pAV2198, pAV2199, and pAV2192) failed to show *rodB1*-complementing activity. Plasmid pAV2186, which contains all of *mreD* and the 5' end of *minC*, and plasmid pAV2186Δ*SspI*, which terminates at the *SspI* site in *mreD* (nucleotide 2679, Fig. 2), both complemented the *rodB1* mutation. Plasmid pAV2186Δ*SspI*Δ*Dra*, which lacks the 5' end of *mreD*, failed to complement. Thus, *rodB1* is allelic to *mreD*, with the mutation upstream of the *DraI* site. To further localize the *rodB1* mutation, we performed similar experiments with PCR products overlapping *rodB* to various extents from the 3' end (Fig. 1C). The results of the complementation studies with plasmid DNA as donor showed that the mutation lies between the *HincII* site 5' to

mreD (start point of plasmids pAV2186 and pAV2186ΔSsp) and the *DraI* site in *mreD* (start point of pAV2186ΔSsp ΔDra). The PCR experiments further localized complementing activity to the start point of pcrdivIVB3771/5365 (nucleotide 2481, Fig. 2).

To determine the nature of the *rodB1* mutation, the mutant allele was subjected to nucleotide sequence analysis. Chromosomal DNA from strain ROD104 was used as template for amplification of the mutant allele by the PCR, and PCR products from three such amplifications were sequenced directly. The product of an additional PCR amplification was used to clone both strands in M13mp18 and M13mp19 and again subjected to nucleotide sequence analysis. In all cases, a G-to-A transition was observed at nucleotide position 2287, resulting in a substitution of a positively charged lysine residue for a negatively charged glutamic acid residue within the N-terminal hydrophobic domain.

Disruption of *mre* genes results in apparent loss of viability. Because of the association of *rodB* and the *E. coli mre* genes with determination of cell shape, it was of interest to examine the effect of insertional inactivation of the *B. subtilis mre* genes on cell morphology. Chromosomal DNA fragments wholly internal to each of the *mre* genes were subcloned into pUC18, and a CAT cassette was inserted into the vector in order to provide selection for Campbell-type insertions (Fig. 1A). Transformation of *B. subtilis* 168 with these plasmids to chloramphenicol resistance occurred at a low frequency (20 to 200 transformants per μg of DNA), and all failed to grow upon subculturing to the same medium used for selection (tryptic soy agar with 5 μg of chloramphenicol per ml). Apparently, insertional inactivation of the *mre* genes leads to loss of viability under these conditions. However, integration of plasmids whose inserts are not contained wholly within an *mre* gene (e.g., pAV2217, pAV2218, and pAV2193), although a low-frequency event, does not lead to loss of viability, since transformants can be subcultured. Examination of these cells with the phase-contrast microscope reveals moderate morphological changes (curved, irregular walls) and a minicell phenotype (38).

Interruption of *minC* or *minD* causes minicell formation. If the *min* gene cluster is functionally analogous to the *minB* operon of *E. coli*, insertional inactivation of either *minC* or *minD* should result in the minicell phenotype (13). To test this hypothesis, plasmids containing chromosomal fragments wholly internal to *minC* or *minD* were integrated into the chromosome of *B. subtilis* 168, resulting in insertional inactivation of the ORF. Clones resulting from transformation with plasmids pAV2211 or pAV2212, which contain inserts internal to *minD*, were found to exhibit a minicell phenotype more severe than that of the *divIVB1* mutant allele (Fig. 8E). When plasmid pAV2210 (*minC*) was transformed into *B. subtilis* 168, minicells, short rods, and filaments were also observed (Fig. 8D). Although the similarity between MinC of *B. subtilis* and MinC of *E. coli* is restricted, the production of minicells resulting from insertional inactivation supports the view that these genes are functional homologs. However, the possibility remains that minicell formation resulted from a polar effect of the insertion in *minC* on transcription of *minD*.

***divIVB1* is allelic to *minD*.** To determine whether *divIVB1* was allelic to one of the genes of the *min* locus, complementation analysis was carried out on strain KUS1101 (*divIVB1*). However, when plasmids containing inserts overlapping the 5' end of *minC* were integrated into the chromosome of KUS1101, all of the resulting merodiploids exhibited the

minicell phenotype. To avoid potential polar effects of integrated plasmids, complementation by congression was performed (see Materials and Methods). As seen in Fig. 1C, complementation was observed with PCR products spanning the region between the *PstI* site in *minC* and the *NdeI* site downstream of *minD*. Therefore, *divIVB1* is allelic to *minC* or *minD*, with the mutation occurring between the *PstI* site in *minC* and the *BglII* site at the 3' terminus of *minD*.

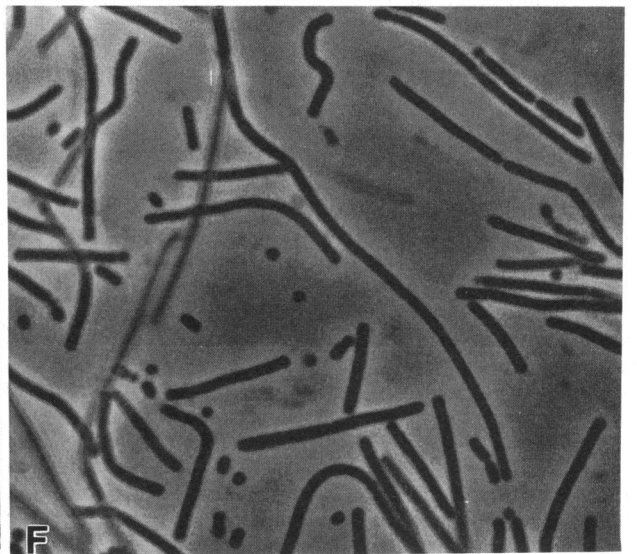
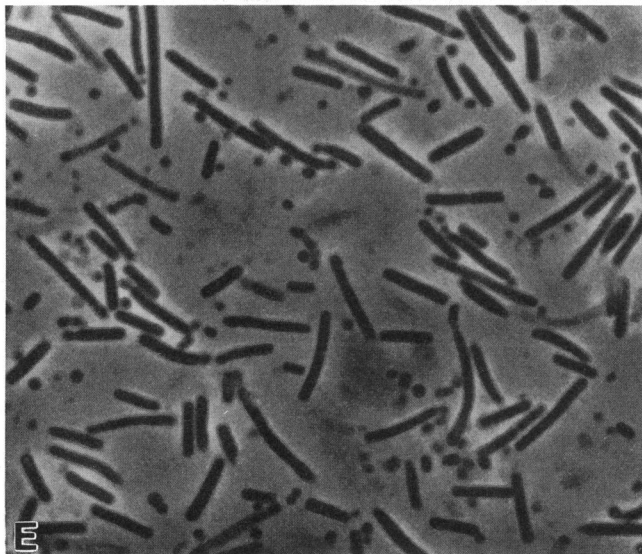
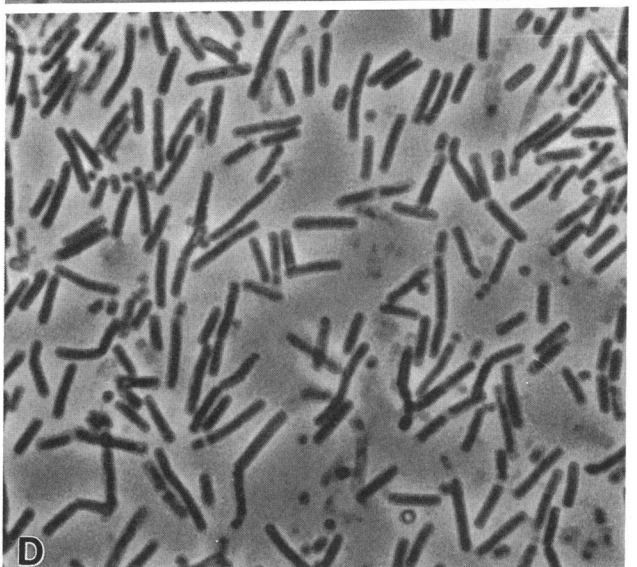
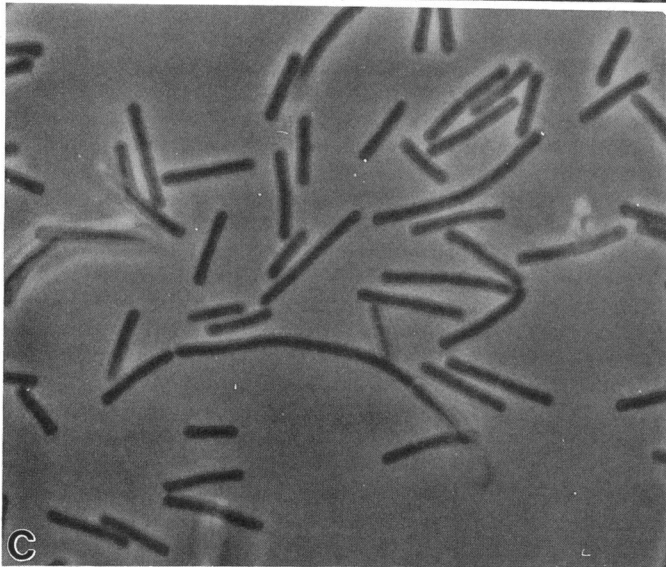
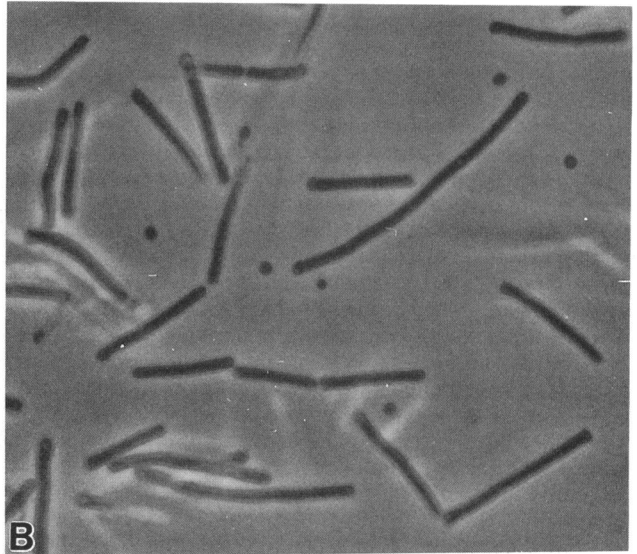
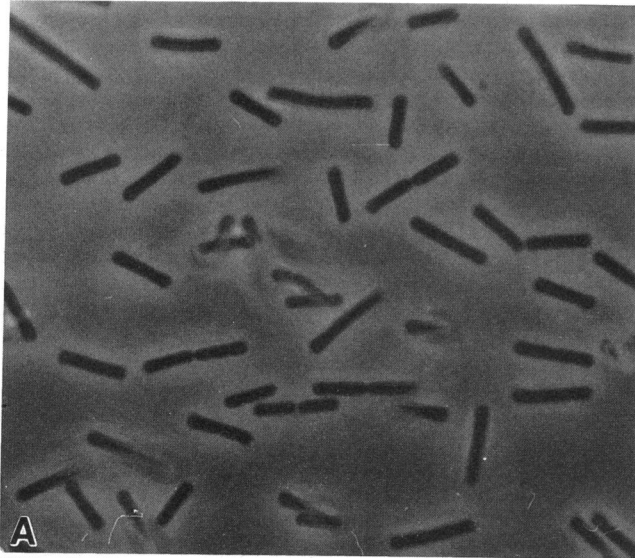
To identify the *divIVB1* mutation, the entire *min* loci of both KUS1101 and CU403 were sequenced by using template generated by the PCR. Both *divIVB1* strains contain two mutations in *minD*. The first mutation is a T-to-A transversion (nucleotide 3751) resulting in the substitution of a lysine for a methionine at amino acid residue 87; the second is a T-to-C transition (nucleotide 3931) resulting in an isoleucine-to-threonine change at amino acid residue 147. Both of the observed mutations in *minD* are within domains highly conserved between the *B. subtilis* and *E. coli* homologs. Although neither mutation occurs at a position of identity between the two species, both occur at positions of conservative substitutions (Fig. 7).

***mre-min* gene clusters may constitute a single operon.** The failure of attempts to map the *divIVB1* mutation by Campbell insertion of plasmids whose inserts overlap the 5' end of *minC* contrasted with results obtained with pAV2148. This plasmid, whose insert continues to the 3' terminus of *minD*, complemented the *divIVB1* phenotype. The low numbers of minicells resulting after integration of pAV2148 were readily explained by sequence analysis, which revealed that subcloning of the *BglII* fragment had destroyed the stop codon of *minD*. Consequently, translation of the plasmid-encoded mRNA would continue into the vector sequence, ostensibly generating a fusion protein with impaired function.

These considerations suggested that the *min* gene cluster may be part of a larger transcription unit. To test this possibility and to determine the extent of the operon, we constructed integrative plasmids spanning various *mre* and/or *min* genes and containing a CAT cassette on the vector. When plasmids overlapping the 5' end of the *min* gene cluster were integrated into the chromosome of *B. subtilis* 168 (e.g., pAV2218 and pAV2219; Fig. 1A), all resulting transformed colonies were found to contain large numbers of minicells, short rods, and filaments (Fig. 8F). Because the resulting merodiploids contained complete copies of all the genes of the *divIVB* region, the minicell phenotype must have resulted from a polar effect on transcription of *minC* and/or *minD*.

In contrast to plasmids overlapping the *min* genes, those overlapping only *mre* genes (e.g., pAV2217, pAV2218, and pAV2193) transformed with low efficiency, probably because interruption of the *mre* gene cluster is not well tolerated. However, all transformants which arose did exhibit a pronounced minicell phenotype. In contrast, integration of pAV2174 yielded transformants which were essentially wild type, though they did produce small numbers of minicells. We conclude that the *mre-min* genes are part of a single transcription unit initiating somewhere between the start codon of *mreB* and the *EcoRI* site immediately upstream.

Presence of the *divIVB* region on plasmids causes minicell formation in *E. coli* and *B. subtilis*. The high level of similarity exhibited between the *E. coli* and *B. subtilis min* homologs suggested the possibility that the *B. subtilis* genes would retain some function in *E. coli*. Phase-contrast microscopy on *E. coli* strains transformed with either pAV2145 or pAV2148 revealed that transformants exhibited a minicell



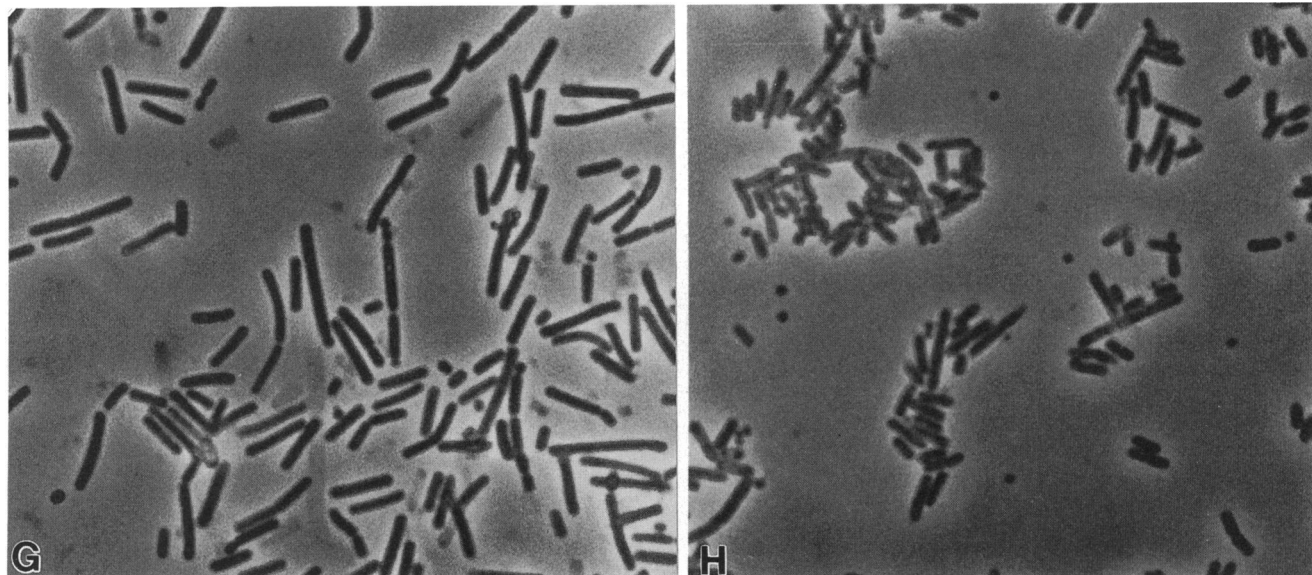


FIG. 8. Phase-contrast micrographs showing complementation and induction of the minicell phenotype by various plasmids. (A) *B. subtilis* 168, wild type; (B) KUS1101, *divIVB1* mutant phenotype; (C) KUS1101 with pAV2148, complementation by the 3.9-kb *Bgl*III fragment; (D) *B. subtilis* 168 with pAV2210, insertional inactivation of *minC*; (E) *B. subtilis* 168 with pAV2211, insertional inactivation of *minD*; (F) *B. subtilis* 168 with pAV2218, polar effect of plasmid insertion immediately upstream of *minC*; (G) *B. subtilis* 168 with pAV2176, mild minicell phenotype of the white colony type; (H) *E. coli* DH5 α (35) with pAV2145; minicell phenotype induced by presence of *divIVB* region on the low-copy-number plasmid.

phenotype (Fig. 8H). However, minicell formation was not observed with all plasmids containing DNA from the *min* locus. Plasmids pAV2176 and pAV2177 do not induce minicell formation in *E. coli*. Significantly, these plasmids contain the *Bgl*III fragment from pAV2145 in the opposite orientation (antisense) with respect to the *lac* promoter on the vector.

The effect of plasmids pAV2176 and pAV2177 on *B. subtilis* 168 was also examined by phase-contrast microscopy. The vector portion of pAV2176 is pMK4 (37), which replicates at a high copy number in *B. subtilis*. The vector portion of pAV2177 is pHP13, which replicates at a low copy number (five or six copies per cell [20]). When transformed into *B. subtilis* 168, the two plasmids induced minicell formation at comparable levels. Moreover, both produced two distinct colony types, one resembling the *divIVB1* colony type (large, translucent, and bluish) and another resembling wild-type colonies (smaller, more opaque, and white). Colonies of the first type exhibited a phenotype indistinguishable from that of *divIVB1* mutants, whereas colonies of the second type produced fewer minicells, and a larger proportion of them were short rods and ovoids (Fig. 8G).

DISCUSSION

The *divIVB* locus contains five genes which appear to constitute two gene clusters based on the function of their *E. coli* homologs. Sequence analysis and preliminary promoter probe studies suggested that promoters precede each gene cluster, with the primary promoter located upstream of *mreB* and a secondary promoter located between *mreD* and *minC* (38). The 3' end of the operon is well defined by the beginning of the *spoIVF* operon and by the presence of a putative rho-independent transcriptional terminator between the stop codon of *minD* and the promoter of *spoIVF* (8). The

5' end is less well defined. In *E. coli*, the *min* and *mre* genes are part of different operons, being separated by nearly half of the *E. coli* chromosome (26 and 71 min, respectively). However, all five ORFs of the *mre-min* region of *B. subtilis* may be part of a single transcription unit. This conclusion is suggested by the observation that Campbell insertion of plasmids overlapping the 5' end of the *min* gene cluster results in minicell formation (e.g., pAV2218), ostensibly by interrupting transcription of the downstream *min* genes. Although Campbell insertions in the *mre* region itself are low-frequency events, they, too, result in formation of minicells (e.g., pAV2217 and pAV2193).

Two observations indicate that the ORF upstream of *mreB* is not part of the *mre-min* transcription unit. First, our results show that Campbell insertions of plasmids into the *mre* region are not well tolerated, suggesting that disruption of the *mre* region results in loss of viability. However, insertions upstream of *mreB* were readily obtained as long as they did not insertional inactivate the upstream genes. Second, the strains generated by Campbell insertion upstream of *mreB* did not show minicell formation at a level corresponding to the *divIVB1* phenotype.

The *mre* and *min* genes, then, may be part of a single operon initiating from a promoter immediately upstream of *mreB* but with an internal secondary promoter upstream of the *min* genes. This arrangement would transcriptionally couple *mre* and *min* gene expression during growth but allow expression of the *min* genes to be regulated independently during division. The reason the *mre* and *min* genes should be transcriptionally coupled in *B. subtilis* but not in *E. coli* may be related to differences in the architecture of gram-positive and gram-negative cell envelopes. The more-prominent peptidoglycan layer in the cell envelopes of gram-positive organisms may necessitate tighter coordination between cell wall synthesis and septum formation.

The most striking observation revealed by sequence analysis of the *min* gene cluster is the absence of a *minE* homolog. A possible explanation is that either *minC* or *minD* performs the function of *minE*. Consistent with this view, the presence of the *divIVB* region on plasmids induces minicell formation in *B. subtilis* and *E. coli*. However, we consider this hypothesis unlikely. Since plasmids bearing the *divIVB* region can induce minicell formation in either *E. coli* or *B. subtilis*, MinD would be the likely candidate for carrying MinE function because of its high degree of conservation. However, the two MinD products are nearly identical in size, with only small nonhomologous regions, making it difficult to envision where the MinE function could reside. Moreover, neither MinC nor MinD exhibits any sequence similarity to MinE. A more likely explanation for the absence of a *minE* homolog in the *divIVB* region is that an added level of control is required by *B. subtilis* because of the necessity of asymmetric septum formation during sporulation. The *minE* homolog in *B. subtilis* may be part of a separate regulatory operon located elsewhere on the chromosome so that it can be regulated separately from *minCD* during sporulation.

Another interesting feature of the *min* sequence is the divergence in the degree of conservation between the MinC and MinD homologs of *B. subtilis* and *E. coli*. MinD is highly conserved over most of its length, whereas MinC shows little conservation except over a very narrow region. These differences may be related to the functions of the two proteins. In *E. coli*, MinD has been shown to serve an accessory role (14). Conservation may be dictated by the requirement that MinD also interact with other regulatory components of the division apparatus. Both MinD polypeptides contain putative nucleotide-binding folds of 10 amino acid residues identical in sequence and position (13, 18), suggesting that MinD may be the target of division regulators. Moreover, MinD has recently been shown to have ATPase activity (11). Finally, both point mutations identified by us in the original *divIVB1* strain (CU403) resulted in amino acid substitutions in highly conserved regions of MinD. In contrast, MinC has been shown to be the actual division inhibitor in *E. coli* (14, 25) and may be expected to interact directly with components of the cell envelope. Differences in the structures of the cell envelopes of gram-positive and gram-negative organisms may dictate the observed divergence of amino acid sequence between the MinC homologs of the two organisms. One expectation of this hypothesis is that the region of MinC which interacts with MinD should be more conserved than the rest of the molecule. Mulder et al. (30) recently identified a series of mutations within *minC* which suppress division inhibition induced by overexpression of *minD*. Significantly, these mutations cluster within the conserved region of MinC.

The observation that the presence of the *divIVB* region on plasmids can induce minicell formation in *E. coli* is intriguing. The high level of homology between the MinD homologs of the two organisms suggests that the minicell phenotype in this case may result from competition between the *B. subtilis* and *E. coli* MinD homologs for MinC. The resulting formation of a nonfunctional hybrid may result in a corresponding drop in the level of functional MinCD. However, minicell formation in *E. coli* was not observed with all plasmids bearing the *divIVB* region. The low-copy-number plasmids pAV2145 and pAV2148 both induced minicell formation, whereas the high-copy-number plasmids pAV2176 and pAV2177 did not. It may be significant that in the low-copy-number plasmids, the insert is in the sense orientation with

respect to the *lac* promoter (on the vector), whereas in the high-copy-number plasmids, it is in the antisense orientation. Since the insert lacks the putative primary promoter upstream of *mreB*, expression would depend either on the *lac* promoter (low-copy-number plasmids only) or on the internal promoter upstream of *minC*. The internal promoter may not be active enough in *E. coli* for the high-copy-number plasmid to produce MinD in sufficient levels to induce minicell formation.

The observation that the presence of the *divIVB* region on plasmids induces minicell formation in *B. subtilis* was unexpected. In the *E. coli* system, overexpression of *minCD* induces filamentation. If the internal promoter upstream of *minC* is functional, one would expect the high-copy-number plasmid to overexpress MinCD and induce filamentation as well. One explanation is that the *E. coli* and *B. subtilis* *min* systems function differently. For example, in *B. subtilis*, formation of an active MinCD may require interaction with an as-yet-unidentified component. If MinCD is present at too high a level, all potential division sites would be occupied by inactive inhibitor, and division would occur randomly at any site. However, the high degree of structural and functional conservation observed among the cell division genes so far identified in the two organisms argues against this view. An alternative explanation is that the MinCD proteins generated from plasmid-derived transcripts are defective. Since the construction of both plasmids resulted in the destruction of the stop codon at the end of *minD*, the resulting fusion protein may no longer be able to inhibit cell division but may still be capable of competing with chromosomally encoded MinCD for binding to division sites. Again, this would result in a nonfunctional MinCD occupying all potential septation sites, and division would occur at all sites with equal frequency. A third, less likely explanation is that the *lac* promoter on the vector may override expression from the internal promoter, resulting in antisense mRNA which would inhibit translation of the wild-type message.

Sequence analysis of the *mre* gene cluster reveals little concrete information on the function of these genes. In *E. coli*, the genes of the *mre* operon (*mreBCD*) are known to be involved in determination of cell shape, since mutation or deletion of the *mre* genes leads to formation of spherical cells. In the case of mutation in *mreB*, this spherical transformation is accompanied by increased expression of *ftsI* and accumulation of its product, pbp3 (septum peptidoglycan synthetase) (40, 41). It has also been proposed that *mreB* is involved in the switch from growth to division because overexpression of *mreB* in wild-type cells leads to cessation of septation. Significantly, we have shown that in *B. subtilis*, the *min* cell division genes appear to be transcriptionally coupled to the *mre* genes.

The high degree of sequence similarity between the *B. subtilis* and *E. coli* *mre* gene products and the similarities of their hydropathy plots suggest that they may have identical functions in the two organisms. Consistent with this view, we show that the *rodB1* mutant allele of *B. subtilis*, which exhibits a temperature-sensitive transition from rod-shaped to spherical cells (23, 33) strictly analogous to that observed with mutation in the *E. coli* *mre* genes, maps to *mreD*. Wachi et al. (39) suggested that the *mre* genes may be membrane-associated regulatory components of cell wall synthesis. Significantly, the *rodB1* mutation results in the substitution of a positively charged lysine for a negatively charged glutamic acid residue within the N-terminal hydrophobic domain of MreD and may be expected to affect insertion or orientation in the cytoplasmic membrane.

We were unable to demonstrate that inactivation of the *mre* genes of *B. subtilis* produced a phenotype analogous to that observed in *E. coli*, because disruption of these genes resulted in loss of viability. Possibly, the *mre* genes serve a more essential function in *B. subtilis* than in *E. coli*. In the latter, deletion of the *mre* genes results in a spherical shape without loss of cell viability, while insertional inactivation of any of the *mre* genes of *B. subtilis* is apparently lethal. Again, this may reflect differences in cell envelope architecture, since gram-positive rods appear to depend on an interaction between peptidoglycan and teichoic acids for stability of the cell envelope. Indeed, mutation at the *rodC* locus, which is involved in teichoic acid synthesis, also results in a spherical shape (21), and insertional inactivation of either of the genes in the *rodC* operon is lethal (42). Work on introducing less-drastic point mutations and in-frame deletions into these genes in order to clarify their function is currently under way.

ACKNOWLEDGMENTS

We thank Richard Losick for communicating sequencing data prior to publication (27) and for sharing preliminary mapping results localizing *rodB1* to the *mre* gene cluster. We also thank John Reeve for strain CU403, Yun Butler for the precursor to pAV2174 (pYB2175), Yamuna Abhayawardhane for confirming the sequence upstream of the leftmost *NdeI* site, and Margaret Hunt for her advice in establishing PCR conditions.

This work was supported by Public Health Service grant GM37990 from the National Institutes of Health.

REFERENCES

- Adler, H. I., W. D. Fischer, A. Cohen, and A. A. Hardigree. 1967. Miniature *Escherichia coli* cell deficient in DNA. Proc. Natl. Acad. Sci. USA 57:321-326.
- Beall, B., M. Lowe, and J. Lutkenhaus. 1988. Cloning and characterization of *Bacillus subtilis* homologs of *Escherichia coli* cell division genes *ftsZ* and *ftsA*. J. Bacteriol. 170:4855-4864.
- Beall, B., and J. Lutkenhaus. 1991. FtsZ in *Bacillus subtilis* is required for vegetative septation and for asymmetric septation during sporulation. Genes Dev. 5:447-455.
- Benton, W. D., and R. W. Davis. 1977. Screening λ gt recombinant clones by hybridization to single plaques in situ. Science 196:180-182.
- Bi, E., and J. Lutkenhaus. 1991. FtsZ ring structure associated with division in *Escherichia coli*. Nature (London) 354:161-164.
- Butler, Y. X. 1991. Ph.D. thesis. University of Kansas, Lawrence.
- Corton, J. C., J. E. Ward, Jr., and J. Lutkenhaus. 1987. Analysis of cell division gene *ftsZ* (*sulB*) from gram-negative and gram-positive bacteria. J. Bacteriol. 169:1-7.
- Cutting, S., S. Roels, and R. Losick. 1991. Sporulation operon *spoIVF* and the characterization of mutations that uncouple mother-cell from forespore gene expression in *Bacillus subtilis*. J. Mol. Biol. 221:1237-1256.
- Dean, D. R., J. A. Hoch, and A. I. Aronson. 1977. Alteration of the *Bacillus subtilis* glutamine synthetase results in overproduction of the enzyme. J. Bacteriol. 131:981-987.
- de Boer, P. A. J., W. R. Cook, and L. I. Rothfield. 1990. Bacterial cell division. Annu. Rev. Genet. 24:249-274.
- de Boer, P. A. J., R. E. Crossley, A. R. Hand, and L. I. Rothfield. 1991. The MinD protein is a membrane ATPase required for the correct placement of the *Escherichia coli* division site. EMBO J. 10:4371-4380.
- de Boer, P. A. J., R. E. Crossley, and L. I. Rothfield. 1988. Isolation and properties of *minB*, a complex genetic locus involved in correct placement of the division site in *Escherichia coli*. J. Bacteriol. 170:2106-2112.
- de Boer, P. A. J., R. E. Crossley, and L. I. Rothfield. 1989. A division inhibitor and a topological specificity factor coded for by the minicell locus determine proper placement of the division septum in *E. coli*. Cell 56:641-649.
- de Boer, P. A. J., R. E. Crossley, and L. I. Rothfield. 1990. Central role for the *Escherichia coli minC* gene product in two different cell division-inhibition systems. Proc. Natl. Acad. Sci. USA 87:1129-1133.
- Doi, M., M. Wachi, F. Ishino, S. Tomioka, M. Ito, Y. Sakagami, A. Suzuki, and M. Matsuhashi. 1988. Determinations of the DNA sequence of the *mreB* gene and of the gene products of the *mre* region that function in formation of the rod shape of *Escherichia coli* cells. J. Bacteriol. 170:4619-4624.
- Erickson, R. J., and J. C. Copeland. 1972. Structure and replication of chromosomes in competent cells of *Bacillus subtilis*. J. Bacteriol. 109:1075-1084.
- Ferrari, F. A., D. Lang, E. Ferrari, and J. A. Hoch. 1982. Molecular cloning of the *spoOB* sporulation locus in bacteriophage lambda. J. Bacteriol. 152:809-814.
- Gill, D. R., G. F. Hatfull, and G. P. C. Salmond. 1986. A new cell division operon in *Escherichia coli*. Mol. Gen. Genet. 205:134-145.
- Gold, L., and G. Stormo. 1987. Translation initiation, p. 1302-1307. In F. C. Neidhardt, J. L. Ingraham, K. B. Low, B. Magasanik, M. Schaechter, and H. E. Umbarger (ed.), *Escherichia coli* and *Salmonella typhimurium*: cellular and molecular biology, vol. 2. American Society for Microbiology, Washington, D.C.
- Haima, P., S. Bron, and G. Venema. 1987. The effect of restriction on shotgun cloning and plasmid stability in *Bacillus subtilis* Marburg. Mol. Gen. Genet. 209:335-342.
- Honeyman, A. L., and G. C. Stewart. 1989. The nucleotide sequence of the *rodC* operon of *Bacillus subtilis*. Mol. Microbiol. 3:1257-1268.
- Innis, M. A., D. H. Gelfand, J. J. Sninsky, and T. J. White (ed.). 1990. PCR protocols: a guide to methods and applications. Academic Press, Inc., New York.
- Karamata, D., M. McConnell, and J. H. Rogers. 1972. Mapping of *rod* mutants of *Bacillus subtilis*. J. Bacteriol. 111:73-79.
- Kyte, J., and R. F. Doolittle. 1982. A simple method for displaying the hydropathic character of a protein. J. Mol. Biol. 157:105-132.
- Lalie, C., F. Bouché, and J.-P. Bouché. 1990. Minicell-forming mutants of *Escherichia coli*: suppression of both DicB- and MinD-dependent division inhibition by inactivation of the *minC* gene product. J. Bacteriol. 172:5852-5855.
- Lerner, C. G., and M. Inouye. 1990. Low copy number plasmids for regulated low-level expression of cloned genes in *Escherichia coli* with blue/white insert screening capability. Nucleic Acids Res. 18:4631.
- Levin, P. A., P. S. Margolis, P. Setlow, R. Losick, and D. Sun. 1992. Identification of *Bacillus subtilis* genes for septum placement and shape determination. J. Bacteriol. 174:6717-6728.
- Lutkenhaus, J. 1990. Regulation of cell division in *E. coli*. Trends Genet. 6:22-25.
- Moran, C. P., Jr., N. Lang, S. Legrice, G. Lee, M. Stephens, A. L. Sonenshein, J. Pero, and R. Losick. 1982. Nucleotide sequences that signal the initiation of transcription and translation in *Bacillus subtilis*. Mol. Gen. Genet. 186:339-346.
- Mulder, E., C. L. Woldringh, F. Tetart, and J.-P. Bouche. 1992. New *minC* mutations suggest different interactions of the same region of division inhibitor MinC with proteins specific for *minD* and *dicB* coinhibition pathways. J. Bacteriol. 174:35-39.
- Narahara, A., K. Naterstad, A. Gronstad, T. Kristensen, R. Lopez, and A. B. Kosltoe. GenBank accession number X62374.
- Pearson, W. R., and D. J. Lipman. 1988. Improved tools for biological sequence comparison. Proc. Natl. Acad. Sci. USA 85:2444-2448.
- Reeve, J. N., N. H. Mendelson, S. I. Coyne, L. L. Hallock, and R. M. Cole. 1973. Minicells of *Bacillus subtilis*. J. Bacteriol. 114:860-873.
- Rosey, E. L., B. Oskouian, and G. C. Stewart. 1991. Lactose metabolism by *Staphylococcus aureus*: characterization of *lacABCD*, the structural genes of the tagatose 6-phosphate pathway. J. Bacteriol. 173:5992-5998.

35. Sambrook, J., E. F. Fritsch, and T. Maniatis. 1989. Molecular cloning: a laboratory manual, 2nd ed. Cold Spring Harbor Laboratory, Cold Spring Harbor, N.Y.
36. Sanger, F., S. Nicklen, and R. Coulson. 1977. DNA sequencing with chain-terminating inhibitors. *Proc. Natl. Acad. Sci. USA* **74**:5463-5467.
37. Sullivan, M. A., R. E. Yasbin, and F. E. Young. 1984. New shuttle vectors for *Bacillus subtilis* and *Escherichia coli* which allow rapid detection of inserted fragments. *Gene* **29**:21-26.
38. Varley, A. W., and G. C. Stewart. Unpublished data.
39. Wachi, M., M. Doi, Y. Okada, and M. Matsuhashi. 1989. New *mre* genes *mreC* and *mreD*, responsible for formation of the rod shape of *Escherichia coli* cells. *J. Bacteriol.* **171**:6511-6516.
40. Wachi, M., M. Doi, S. Tamaki, W. Park, S. Nakajima-Iijima, and M. Matsuhashi. 1987. Mutant isolation and molecular cloning of *mre* genes which determine cell shape, sensitivity to mecillinam, and amount of penicillin-binding proteins in *Escherichia coli*. *J. Bacteriol.* **169**:4935-4940.
41. Wachi, M., and M. Matsuhashi. 1989. Negative control of cell division by *mreB*, a gene that functions in determining the rod shape of *Escherichia coli* cells. *J. Bacteriol.* **171**:3123-3127.
42. Wagner, P. M., and G. C. Stewart. 1991. Role and expression of the *Bacillus subtilis* *rodC* operon. *J. Bacteriol.* **173**:4341-4346.